Porous Dye Affinity Beads for Nickel Adsorption from Aqueous Solutions: A Kinetic Study

Sinan Akgöl,[1] Erdal Kuşvuran,[2] Ali Kara,[3] Serap Şenel,[1] Adil Denizli[1]

[1]*Chemistry Department, Hacettepe University, Beytepe, Ankara, Turkey*
[2]*Chemistry Department, Çukurova University, Balcalı, Adana, Turkey*
[3]*Chemistry Department, Uludağ University, Bursa, Turkey*

Received 10 March 2005; accepted 17 October 2005
DOI 10.1002/app.23856
Published online in Wiley InterScience (www.interscience.wiley.com).

ABSTRACT: We investigated a new adsorbent system, Reactive Red 120 attached poly(2-hydroxyethyl methacrylate ethylene dimethacrylate) [poly(HEMA–EDMA)] beads, for the removal of Ni^{2+} ions from aqueous solutions. Poly(HEMA–EDMA) beads were prepared by the modified suspension copolymerization of 2-hydroxyethyl methacrylate and ethylene dimethacrylate. Reactive Red 120 molecules were covalently attached to the beads. The beads (150–250 μm), having a swelling ratio of 55% and carrying 25.5 μmol of Reactive Red 120/g of polymer, were used in the removal of Ni^{2+} ions. The adsorption rate and capacity of the Reactive Red 120 attached poly(HEMA–EDMA) beads for Ni^{2+} ions was investigated in aqueous media containing different amounts of Ni^{2+} ions (5–35 mg/L) and having different pH values (2.0–7.0). Very high adsorption rates were observed at the beginning, and adsorption equilibria were then gradually achieved in about 60 min. The maximum adsorption of Ni^{2+} ions onto the Reactive Red 120 attached poly(HEMA–EDMA) beads was 2.83 mg/g at pH 6.0. The nonspecific adsorption of Ni^{2+} ions onto poly(HEMA–EDMA) beads was negligible (0.1 mg/g). The desorption of Ni^{2+} ions was studied with 0.1*M* HNO_3. High desorption ratios (>90%) were achieved. The intraparticle diffusion rate constants at various temperatures were calculated as $k_{20°C} = 0.565$ mg/g $min^{0.5}$, $k_{30°C} = 0.560$ mg/g $min^{0.5}$, and $k_{40°C} = 0.385$ mg/g $min^{0.5}$. Adsorption–desorption cycles showed the feasibility of repeated use of this novel adsorbent system. The equilibrium data fitted very well both Langmuir and Freundlich adsorption models. The pseudo-first-order kinetic model was used to describe the kinetic data. © 2006 Wiley Periodicals, Inc. J Appl Polym Sci 100: 5056–5065, 2006

Key words: adsorption; dyes/pigments; chromatography

INTRODUCTION

The industrial usage of nickel compounds includes nickel refining, electroplating, stainless steel production, and nickel–cadmium batteries. Moreover, the combustion of fossil fuels and the incineration of nickel-containing solid waste cause the spreading of nickel-containing aerosols in the surrounding environments and in the workplace.[1] Natural sources of atmospheric nickel include dust from volcanic emissions and the weathering of rocks and soils. Natural sources of aqueous nickel include biological cycles and the solubilization of nickel compounds from soils. The global input of nickel into the human environment is approximately 150,000 metric tons per year from natural sources and 180,000 metric tons per year from anthropogenic sources, including emissions from fossil-fuel consumption and the industrial production, use, and disposal of nickel compounds and alloys.

Exposure to nickel compounds can produce a variety of adverse effects on human health.[2] A nickel allergy in the form of contact dermatitis is the most common reaction. Although the accumulation of nickel in the body through chronic exposure can lead to lung fibrosis and cardiovascular and kidney diseases, the most serious concerns are related to nickel's carcinogenic activity. The molecular mechanism of nickel-induced carcinogenesis is not fully understood. Several cellular pathways have been proposed to explain this process.[3] They include promutagenic DNA damage (oxidative damage to nucleobases and DNA strand breaks).[4]

The high consumption of nickel-containing products inevitably leads to environmental pollution by nickel and its derivatives at all stages of production, utilization, and disposal. A number of technologies have been used to remove Ni^{2+} ions from wastewater streams, such as adsorption onto activated carbon,[5] filtration of precipitate,[6] and crystallization in the form of nickel carbonate.[7] In the last decade, adsorption has been shown to be an effective and economically feasible alternative method for the removal of heavy-metal ions such as Ni^{2+} ions.[8] Specific polymeric sorbents consist of a metal-chelating ligand that interacts with the heavy-metal ions specifically and a carrier matrix that may be an inorganic material (e.g.,

Correspondence to: A. Denizli (denizli@hacettepe.edu.tr).

aluminum oxide, silica, activated carbon, or glass) or polymer beads [e.g., polystyrene, cellulose, poly(maleic anhydride), or poly(methyl methacrylate)].[9] A large number of chelating polymers incorporating a variety of ligands [e.g., poly(ethylene imine), iminodiacetic acid, thiazolidine, and methacryloylamidohistidine] have been prepared, and their analytical properties have been investigated.[10–14]

In this study, the removal of Ni^{2+} ions with Reactive Red 120 attached poly(2-hydroxyethyl methacrylate ethylene dimethacrylate) [poly(HEMA–EDMA)] was investigated. Poly(HEMA–EDMA) beads (150–250 μm) were produced by the suspension copolymerization of 2-hydroxyethyl methacrylate (HEMA) and ethylene dimethacrylate (EDMA). The dichlorotriazine dye Reactive Red 120 was attached covalently as a new dye ligand. The adsorption and desorption of Ni^{2+} from aqueous media were studied. The adsorption conditions (e.g., Ni^{2+}-ion concentration and pH) were varied to evaluate their effects on the performances of Reactive Red 120 attached chelating beads. In addition, the equilibrium data fitted very well both Langmuir and Freundlich adsorption models. The pseudo-first-order model was used to describe the kinetic data.

EXPERIMENTAL

Chemicals

HEMA (Sigma Chemical Co., St. Louis, MO) and EDMA (Aldrich, Munich, Germany) were distilled *in vacuo* (100 mmHg). Reactive Red 120 was also obtained from Sigma Chemical and was used without further purification. Poly(vinyl alcohol) (molecular weight = 100.000, 98% hydrolyzed) was purchased from Aldrich. α,α'-Azobisisobutyronitrile (AIBN) was obtained from Fluka A.G. (Buchs, Switzerland) and used as received. All other chemicals were of the highest purity commercially available and were used without further purification. All water used in the experiments was purified with a Barnstead (Dubuque, IA) ROpure LP reverse-osmosis unit with a high-flow cellulose acetate membrane (Barnstead D2731) followed by a Barnstead D3804 NANOpure organic/colloid removal and ion-exchange packed bed system.

Preparation of the poly(HEMA–EDMA) beads

A porous, crosslinked copolymer was prepared by the reaction of HEMA and EDMA by a procedure given in detail elsewhere.[15] To obtain polymeric beads with an average diameter of 150–200 μm, the following experimental recipe was used: the dispersion medium was prepared through the dissolution of 200 mg of poly(vinyl alcohol) in 50 mL of distilled water. Toluene (12 mL) was mixed with 4 mL of HEMA and 8 mL of EDMA, and then 60 mg of AIBN was added. This monomer phase was then transferred into the dispersion medium placed in a glass polymerization reactor (100 mL), which was in a thermostatic water bath. The polymerization medium was magnetically stirred at 600 rpm. The reactor was flushed with bubbling nitrogen and then was sealed. The mixture was reacted at 65°C for 4 h and then at 90°C for 2 h. The beads were collected by filtration under suction and washed sequentially with water and ethyl alcohol and were dried in a vacuum oven at 60°C for 48 h.

Dye incorporation to the poly(HEMA–EDMA) beads

To have the beads carrying dye, the following procedure was applied: 10 mL of an aqueous solution containing Reactive Red 120 (2.0 mg/mL) was poured into 90 mL of a suspension of the beads in purified water (containing 3.0 g of the beads), and then 4.0 g of NaOH was added. The medium was heated in a sealed reactor for 4 h at 400 rpm and then at 80°C. Under these experimental conditions, a nucleophilic substitution reaction took place between the chlorine-containing group of Reactive Red 120 and the hydroxyl groups of the HEMA monomer, with the elimination of NaCl, resulting in the covalent attachment of Reactive Red 120 onto the beads. The covalent coupling of Reactive Red 120 to the poly(HEMA–EDMA) beads resulted from the formation of an ether linkage between the reactive triazine ring of the dye and the hydroxyl groups of HEMA. Any remaining chlorine atoms in the dye-attached beads due to the dichlorotriazinyl dye structure, after covalent immobilization, were converted to amino groups by treatment with 2*M* NH_4Cl at pH 8.5 for 24 h at room temperature. The dye-attached beads were filtered and washed sequentially with distilled water and methanol several times until all the unbound dye was removed. Reactive Red 120 attached poly(HEMA–EDMA) beads were stored at 4°C with 0.02% sodium azide to prevent microbial contamination.

Characterization of the beads

The water uptake ratio of the beads was determined in distilled water. The experiment was conducted as follows. Initially dry beads were carefully weighed before being placed in a 50-mL vial containing distilled water. The vial was put into an isothermal water bath at 25°C for 24 h. The beads were taken out from water, wiped with filter paper, and weighed. The mass ratio of dry and wet samples was recorded. The water content of the beads was calculated with the following expression:

$$\text{Water uptake ratio (\%)} = [(W_s - W_0)/W_0] \times 100 \quad (1)$$

where W_0 and W_s are the masses of poly(HEMA–EDMA) beads before and after the uptake of water, respectively.

The morphology of a cross section of the dried beads was investigated with a scanning electron microscope (JEM 1200 EX, JEOL, Tokyo, Japan). The beads were dried in a vacuum oven at 50°C for 24 h. Pore volumes and an average pore diameter greater than 20 Å were determined with a mercury porosimeter up to 2000 kg/cm^2 with a Carlo Erba (Milan, Italy) model 200. The specific surface area of the beads was determined in the Brunauer–Emmett–Teller (BET) isotherm of nitrogen with an ASAP2000 instrument (Micromeritics, Norcross, VA). Fourier transform infrared (FTIR) spectra of the Reactive Red 120, poly(HEMA–EDMA) beads, and Reactive Red 120 attached poly(HEMA–EDMA) beads were obtained with an FTIR spectrophotometer (FTIR 8000 series, Shimadzu, Tokyo, Japan). The dry beads (ca. 0.1 g) were thoroughly mixed with KBr (0.1 g, IR-grade, Merck, Darmstadt, Germany) and pressed into a tablet, and the spectrum was then recorded. To evaluate the Reactive Red 120 loading, the poly(HEMA–EDMA) beads were subjected to elemental analysis with a Leco (St. Joseph, MI) CHNS-932 elemental analyzer.

Adsorption–desorption studies with Ni^{2+} ions

The adsorption of Ni^{2+} ions from aqueous solutions was investigated in batch adsorption equilibrium experiments. The effects of the initial concentration of Ni^{2+} ions and pH of the medium on the adsorption rate and capacity were studied. Aqueous solutions (10 mL) containing different amounts of Ni^{2+} ions (in the range of 5–35 mg/L) were treated with the adsorbents [the plain and dye-attached poly(HEMA–EDMA)] at different pHs (in the range of 2.0–7.0) at room temperature in flasks agitated magnetically at an agitation speed of 600 rpm. After adsorption, the polymeric beads were separated from the adsorption medium by filtration. The concentration of Ni^{2+} ions in the aqueous solution phases after the desired treatment periods were measured with a Hitachi 180-80 polarized Zeeman atomic absorption spectrophotometer (Tokyo, Japan) with an air–acetylene flame. Nickel hollow cathode lamp was used. The metal adsorption capacity was found with the mass balance.

The desorption of Ni^{2+} ions was studied with 0.1*M* HNO_3 at pH 1.0. The beads carrying Ni^{2+} ions were placed in this desorption medium and stirred (at a stirring rate of 600 rpm) for 2 h at room temperature. The final Ni^{2+}-ion concentration in the aqueous phase was determined with an atomic absorption spectrophotometer. The desorption ratio was calculated from the amount of Ni^{2+} ions adsorbed onto the beads and the final Ni^{2+}-ion concentration in the desorption medium. To determine the reusability of the Reactive Red 120 attached poly(HEMA–EDMA) beads, the adsorption–desorption cycle was repeated 10 times with the same sorbent.

Equilibrium modeling

The Langmuir and Freundlich adsorption isotherm models were used for describing the adsorption isotherm.[16,17] The linear equations of Langmuir [eq. (2)] and Freundlich [eq. (3)] are represented as follows:

$$C_e/Q = (1/Q_0b) + C_e/Q_0 \quad (2)$$

$$\ln Q = 1/n(\ln C_e) + \ln K_F \quad (3)$$

where b is the Langmuir isotherm constant, C_e is the equilibrium concentration, Q is the adsorption capacity, Q_0 is the maximum adsorption capacity, K_F is the Freundlich constant, and n is the Freundlich exponent. The ratio of Q_0 gives the theoretical monolayer saturation capacity of Reactive Red 120 attached poly(HEMA–EDMA) beads. The essential characteristic of the Langmuir equation can be expressed in terms of the dimension factor, R_L, which was defined by Mc Kay et al.[18] as follows:

$$R_L = 1/(1 + bC_0) \quad (4)$$

where C_0 is the initial metal concentration (mg/L) and b is the Langmuir constant. The value of R_L indicates the shape of the isotherms to be unfavorable ($R_L > 1$), linear ($R_L = 1$), favorable ($0 < R_L < 1$), or irreversible ($R_L = 0$).

Kinetic modeling

To investigate the mechanism of adsorption, the pseudo-first-order model, pseudo-second-order model, and intraparticle diffusion model were used for testing dynamic experimental data.[19–21] The pseudo-first-order model of Lagergren is given as follows:

$$\log(q_e - q_t) = \log q_e - K_1t/2.303 \quad (5)$$

The intraparticle diffusion equation can be described as follows:

$$q_t = k_it^{0.5} \quad (6)$$

where K_1 is the rate constant of pseudo-first-order adsorption (1/min) and k_i is the intraparticle diffusion rate constant (mg/g min$^{0.5}$). q_e and q_t are the amounts of metal adsorbed on the adsorbent (mg/g) at equilibrium and at time t, respectively.

RESULTS AND DISCUSSION

Poly(HEMA–EDMA) (150–250 μm) beads carrying Reactive Red 120 were prepared as affinity adsorbents for nickel removal. The main selection criteria of poly(HEMA–EDMA) are its mechanical strength and chemical stability. The hydrophilic poly(HEMA–EDMA) beads were crosslinked structures. They did not dissolve in aqueous media but did swell, depending on the degree of crosslinking.[22] The equilibrium swelling ratio (the ratio of the weights of the beads before and after swelling) of the beads was 55%. These swollen beads had an average diameter within the range of 150–250 μm. These dye-attached beads were suitable for packed or fluidized bed column applications.

According to the mercury porosimetry data, the pore radii of the poly(HEMA–EDMA) beads changed between 175 and 400 nm. This indicated that the beads contained mainly macropores. This pore diameter range was possibly available for the diffusion of nickel ions. The ionic diameter of Ni^{2+} ions was 0.138 nm. On the basis of these data, we concluded that the beads had effective pore structures for the diffusion of Ni^{2+} ions.

The surface area of the beads was found to be 56 m^2/g by the BET method. After Reactive Red 120 attachment, the specific surface area was found to be the same. Therefore, these pores were not blocked by dye molecules.

The surface morphology and internal structure of the poly(HEMA–EDMA) beads are shown by electron micrographs in Figure 1, which shows that the beads were spherical and had a rough surface. Figure 1(b) was taken with broken beads so that we could observe the internal part. The presence of macropores within the bead interior can be clearly seen in this photograph. It can be concluded that the poly(HEMA–EDMA) beads had a macroporous interior surrounded by a reasonably rough surface in the dry state. The roughness of the bead surface should be considered a factor increasing the specific surface area. In addition, these macropores reduced the diffusional resistance and facilitated mass transfer because of the microporous structure. This also provided higher Reactive Red 120 attachment and enhanced the nickel adsorption capacity.

Poly(HEMA–EDMA) can be fairly reactive in nucleophilic substitution reactions via free alcoholic —OH groups, and a chemical bond occurs if the substrate has a leaving group suitable for a substitution reaction as chloro atoms. Thus, an adsorbent can be yielded containing aromatic groups, such as dye molecules; in particular, Reactive Red 120 has a lot of aromatic structure. Figure 2 shows FTIR spectra of plain and modified beads. In the spectrum for Reactive Red 120 [Fig. 2(b)], the absorption bands from

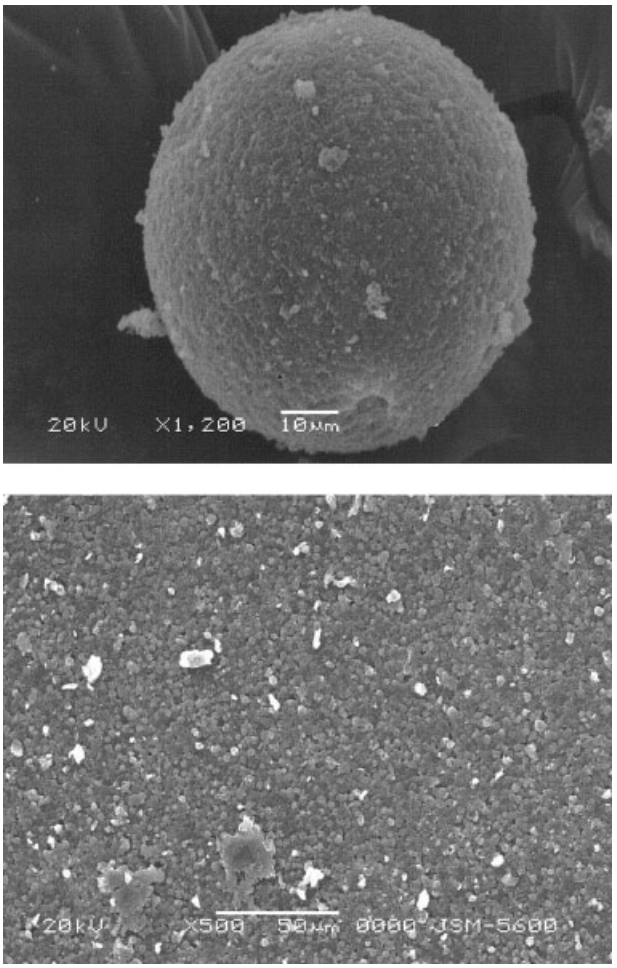

Figure 1 Surface morphology and internal structure of the poly(HEMA–EDMA) beads.

1324 to 1617 cm^{-1} correspond to the vibration of aryl C═C bonds. Reactive Red 120 consists of two naphthalene rings, three aniline groups, and two triazine rings, and the absorption bands in this region therefore overlap because of the high intensity of the absorption bands of their C═C bond aromatic rings. The broad peak near 3446 cm^{-1} indicated N—H and phenolic —O—H groups. The 1203- and 1045-cm^{-1} absorption bands refer to SO_2 asymmetric stretching and S═O vibrations.

The absorption bands of the functional groups of poly(HEMA–EDMA) can be clearly seen in Figure 2(c). Absorption bands at 3466 and 2987/2955 cm^{-1} are due to the stretching of alcoholic —OH and aliphatic CH_2/CH_3, respectively. The intensive peak at 1727 cm^{-1} corresponds to the C═O group. The 1457- and 1370-cm^{-1} peaks are absorption bands of $(CH_3)_2C$— stretching. C—H out-of-plane stretching absorbs IR radiation at 1263 and 1158 cm^{-1}, and C—O—C also does at 1158 cm^{-1}.

When spectra of poly(HEMA–EDMA) and Reactive Red 120 attached poly(HEMA–EDMA) are compared,

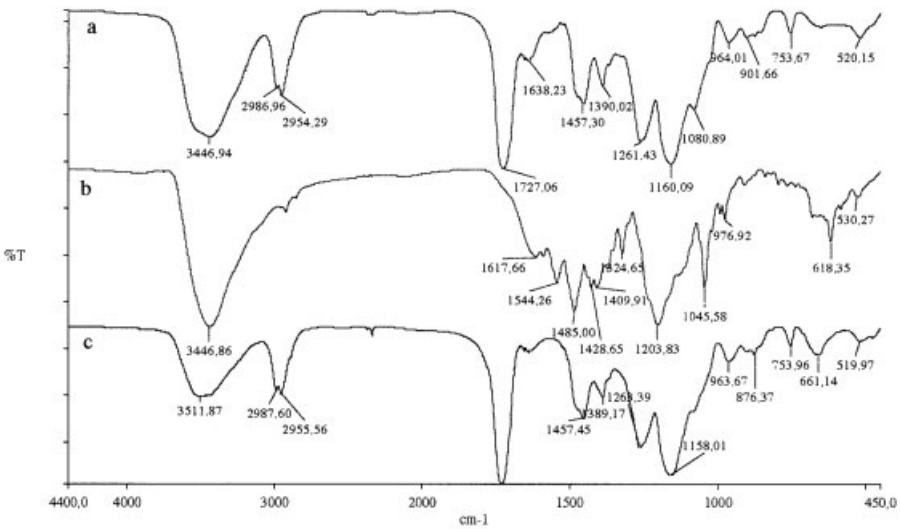

Figure 2 FTIR spectra of (a) Reactive Red 120 attached poly(HEMA–EDMA), (b) Reactive Red 120, and (c) poly(HEMA–EDMA).

the major differences are the disappearance of C—Cl absorption bands and the enhanced intensity of the 3446-cm^{-1} peak, which refer to N—H, phenol —OH, and nonbonding alcoholic —OH. On the other hand, although the ratio of the 3511-cm^{-1} peak to the 2987- or 2955-cm^{-1} peaks is almost equal to the one in Figure 2(a), this ratio is bigger than the one in Figure 2(c) because N—H and phenol —OH bonds enhance the intensity of the absorption band.

Reactive Red 120 is a dichlorotriazine dye (Fig. 3), and it contains six sulfonate groups, four secondary amino groups, and two hydroxyl groups. The binding of the dye ligands to metal ions may have resulted in ion-exchange interactions. The Reactive Red 120 molecules were covalently attached to the poly(HEMA–EDMA) beads. It is accepted that ether linkages are formed between the reactive triazine ring of the dye and the hydroxyl groups of the adsorbent. The Reactive Red 120 attached beads were extensively washed to ensure that there was no dye leakage from any of the dye-attached beads and in any media used at adsorption or desorption steps.

Effect of the initial Ni^{2+} concentration on the adsorption

The adsorption capacities of Ni^{2+} ions investigated on the Reactive Red 120 attached poly(HEMA–EDMA) beads are given in Figure 4 as a function of the initial concentration of Ni^{2+} ions within the aqueous phase. The nonspecific adsorption of Ni^{2+} ions onto poly(HEMA–EDMA) beads was negligible (0.1 mg/g). The Ni^{2+}-ion adsorption capacity of the Reactive Red 120 attached poly(HEMA–EDMA) beads increased first with an increasing initial concentration of Ni^{2+} ion and then reached a saturation level. The maximum adsorption capacity of the Reactive Red 120 attached poly(HEMA–EDMA) beads was 2.83 mg/g for Ni^{2+} ions. This capacity level may have been due to the presence of functional chelating groups on the dye-attached polymeric beads. The specificity of the metal-chelating ligand (i.e., Reactive Red 120 molecules) may also contribute to this high adsorption capacity.

Figure 5 shows equilibrium adsorption times of the Ni^{2+} ions on the Reactive Red 120 attached poly(HEMA–EDMA) beads from aqueous solutions at a constant pH of 6.0. The metal-ion adsorption capacity increased with time during the first 60 min. Data on the adsorption kinetics of different heavy-metal ions, including Ni^{2+} ions by various polymer sorbents, have shown a wide range of adsorption rates. Veglio et al.[23] studied the adsorption of Cu^{2+} ions by calcium alginate beads, and they reported that the kinetics of the resin–metal interaction was rather slow. The authors reported equilibrium contact times ranging be-

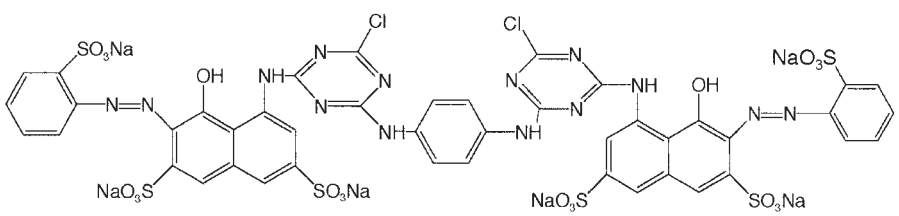

Figure 3 Chemical structure of Reactive Red 120.

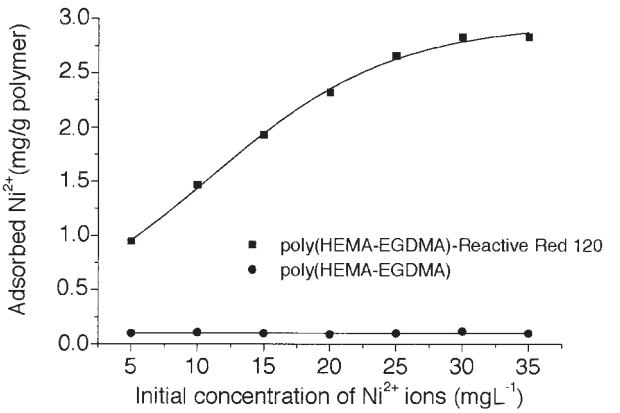

Figure 4 Effect of the initial concentration of Ni^{2+} adsorption onto poly(HEMA–EDMA) beads (dye loading = 25.5 μmol/g, pH = 6.0, temperature = 30°C).

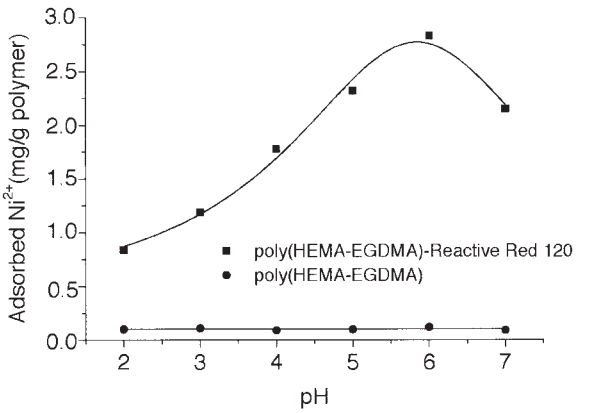

Figure 6 Effect of pH on the adsorption of Ni^{2+} ions on Reactive Red 120 attached poly(HEMA–EDMA) beads (dye loading = 25.5 μmol/g, Ni^{2+} concentration = 30 mg/L, temperature = 30°C).

tween 2 and 24 h. Gupta et al.[24] studied Hg^{2+} adsorption on composites of polyaniline with polystyrene. They showed that adsorption was fast and a complete equilibrium between the two phases was established in 40 min. Zhou et al.[25] studied the adsorption of heavy-metal ions, including Pb^{2+}, Cu^{2+}, and Cd^{2+}, on a blend of cellulose/chitin beads. The time required to reach an equilibrium state was 4–5 h. Latha et al.[26] studied ethylenediamine-functionalized polyacrylamide resin for the extraction of Ni^{2+} ions, and they reported that the complexation reaction proceeded very slowly (the equilibrium time was 5 h). Li and Bai[27] studied the adsorption of Cu^{2+} by chitosan–cellulose hydrogel beads, and they reported that the adsorption equilibrium was reached at about 7 h for the crosslinked chitosan–cellulose beads. Many experimental and structural parameters determine the adsorption rate, such as the stirring rate in the aqueous phase, structural properties of the sorbent (e.g., porosity, surface area, topography, and swelling degree), amount of the sorbent, ion properties (e.g., hydrated ionic radius and coordination number), initial concentration of heavy-metal ions, chelate-formation rates between the complexing ligand and the metal ions, and existence of other metal ions that may compete with the metal ions of interest for the same active complexation sites. Therefore, a comparison of the adsorption rates reported is too difficult to achieve. However, the adsorption rates obtained with the Reactive Red 120 attached poly(HEMA–EDMA) beads produced seem to be good.

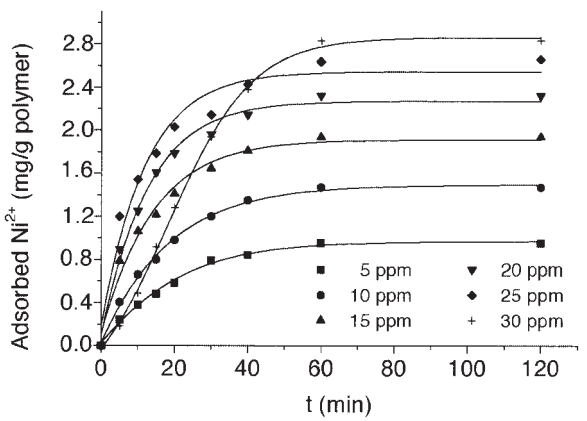

Figure 5 Equilibrium adsorption time of the Ni^{2+} ions on Reactive Red 120 attached poly(HEMA–EDMA) beads (dye loading = 25.5 μmol/g, pH = 6.0, temperature = 30°C).

Effect of pH

Because of the protonation and deprotonation of the acidic and basic groups of the metal complexation ligand (dye molecules), the sorption behavior for metal ions is influenced by the pH value, which affects the surface structure of the sorbents, the formation of metal ions, and the interaction between the sorbents and metal ions. Therefore, the pH dependence of the adsorption for metal ions was investigated in detail. Figure 6 shows the pH profile data for Ni^{2+}-ion adsorption. The nonspecific adsorption of Ni^{2+} ions onto poly(HEMA–EDMA) beads was negligible (0.1 mg/g). This figure shows that the complexation behavior of Ni^{2+} ions is sensitive to pH changes, especially at a lower pH region. The inhibition of metal chelation with a decrease in pH was observed by several authors and in different adsorbents.[28,29] Thus, protons and metal ions appear to compete for the same binding sites. The adsorption capacities increased with increasing pH, reaching plateau values around pH 6.0. High adsorption at relatively high pH values implies that metal ions interact with different metal-chelating ligands, including dyes such as Cibacron Blue F3GA (unprotonated) molecules by chelation.[30–32]

Pore diffusion studies

According to previous studies, a plot of q_t versus $t^{0.5}$ may present multilinearity.[33] The first linear portion is the external surface adsorption stage. The second portion is the gradual adsorption stage, in which the intraparticle diffusion is rate-controlled. The third portion is the final equilibrium stage.[34] The effects of the diffusion rate on intraparticle diffusion are given in Figure 7. When the adsorption of the exterior surface reached saturation, the metal ions entered the poly(HEMA–EDMA) particles through the pores within the particle and were adsorbed by the interior surface of the particle. During the adsorption of Ni^{2+} ions onto Reactive Red 120 attached poly(HEMA–EDMA) beads, only one line for each temperature was obtained, and this indicates that both external surface and interior surface adsorption took place during the adsorption process. The intraparticle diffusion rate constants at various temperatures were calculated (from Fig. 6) as $k_{20°C}$ = 0.565 mg/g $min^{0.5}$, $k_{30°C}$ = 0.560 mg/g $min^{0.5}$, and $k_{40°C}$ = 0.385 mg/g $min^{0.5}$. When intraparticle diffusion rate constants were compared, inverse proportionality was observed. With increasing temperature, the kinetic energy of Ni^{2+} in solution was enhanced, probably along with diffusion into pores, because Ni^{2+} adsorption is exothermic in nature. Therefore, the diffusion rate decreased with increasing temperature.

Desorption and reusability

To be useful in metal-ion-recycling processes, metal ions adsorbed should be easily desorbed under suitable conditions. Adsorbents should be used many times to decrease material cost. Desorption experiments were performed with a 0.1*M* HNO_3 (pH 1.0) solution as the desorption agent. The desorption of the adsorbed Ni^{2+} ions from the Reactive Red 120 attached poly(HEMA–EDMA) beads was studied in a batch experimental setup. The dye-attached beads carrying the maximum amounts of the respective Ni^{2+} ions were placed within the desorption medium containing 0.1*M* HNO_3 (pH 1.0), and the amount of Ni^{2+} ions desorbed in 2 h was measured. The desorption ratio was then calculated. Desorption ratios were very high (up to 90%) with the desorption agent under the conditions used for Ni^{2+} ions. To obtain the reusability of the Reactive Red 120 attached poly(HEMA–EDMA) beads, the adsorption–desorption cycle was repeated five times with the same adsorbent. As shown in Figure 8, the adsorption capacity of the sorbent for Ni^{2+} ions did not significantly change during the repeated adsorption–desorption operations.

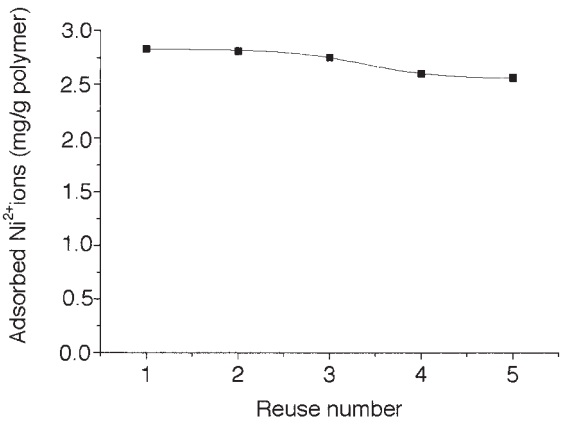

Figure 8 Desorption and reusability of Reactive Red 120 attached poly(HEMA–EDMA) beads (dye loading = 25.5 μmol/g, Ni^{2+} concentration = 30 mg/L, pH = 6.0, temperature = 30°C).

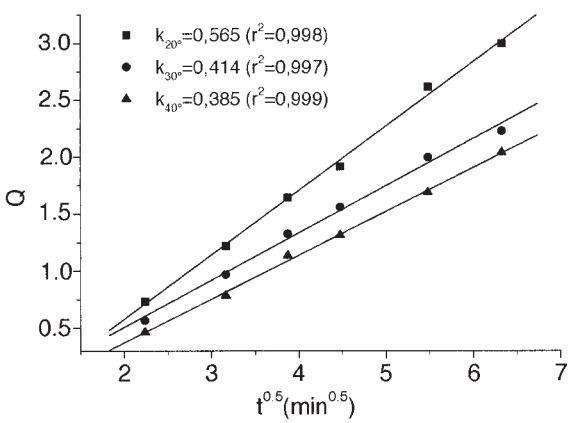

Figure 7 Effect of pore diffusion studies of Ni^{2+} adsorption on Reactive Red 120 attached poly(HEMA–EDMA) beads at various temperatures (dye loading = 25.5 μmol/g, Ni^{2+} concentration = 30 mg/L, pH = 6.0).

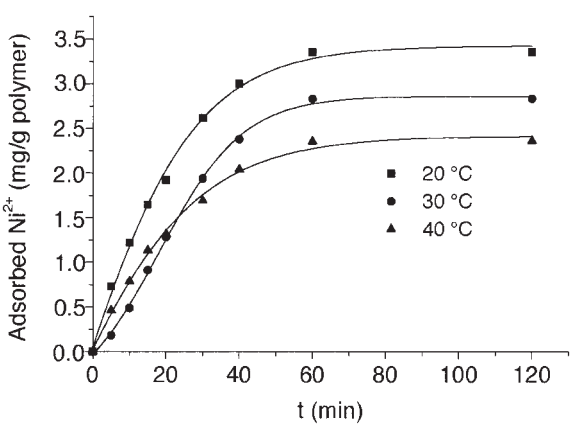

Figure 9 Adsorption of Ni^{2+} on Reactive Red 120 attached poly(HEMA–EDMA) beads at various temperatures (dye loading = 25.5 μmol/g, Ni^{2+} concentration = 30 mg/L, pH = 6.0).

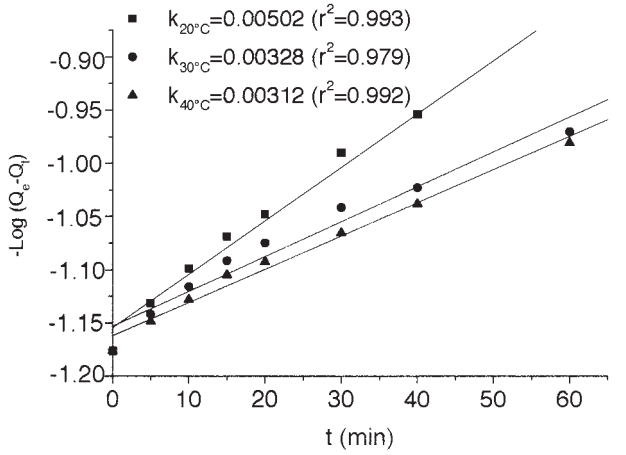

Figure 10 Linear transforms of $\log(Q_e - Q_t)$ versus time at various temperatures for the adsorption of Ni^{2+} ions (dye loading = 25.5 μmol/g, Ni^{2+} concentration = 30 mg/L, pH = 6.0).

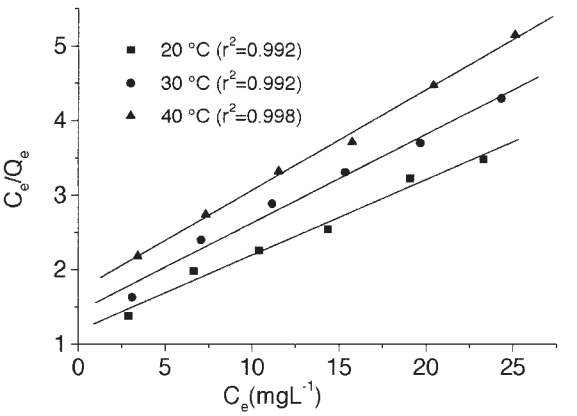

Figure 11 Establishment of the Langmuir monolayer adsorption constant for the adsorption of Ni^{2+} on Reactive Red 120 attached poly(HEMA–EDMA) beads (dye loading = 25.5 μmol/g, pH = 6.0).

Adsorption kinetics

In this section, the change in the adsorption capacity with a rise in temperature is examined (Fig. 9). As can be seen in Figure 9, the adsorption capacity and temperature were inversely proportional. At the end of 60 min, the amounts of Ni^{2+} adsorbed onto Reactive Red 120 attached poly(HEMA–EDMA) beads were 3.35, 2.83, and 2.44 mg/g of polymer at 20, 30, and 40°C, respectively. Figure 10 shows the linear transforms of $\log(Q_e - Q_t)$ versus time at various temperatures for the adsorption of Ni^{2+} ions. Linear transforms and regression coefficients were determined in Figure 10. Regression coefficients of points obtained from the pseudo-first-order relation were greater than 0.970.

The adsorption kinetic constants as pseudo-first-order kinetic constants are given in Table I.

Adsorption isotherms

The adsorption isotherms were studied at various temperatures. A plot of the linear Langmuir equation C_e/Q_e versus C_e is shown in Figure 11. The values of the isotherm constants (including Q_0) of linear regression are given in Table II. The adsorption capacities of Reactive Red attached poly(HEMA–EDMA) decreased with increasing temperature. Q_0 was determined to be 9.88 mg/g for Ni^{2+} at 30°C. The plots in Figure 11 show that the Langmuir equation provides an accurate description of the experimental data; this is further confirmed by the extremely high values of the correlation coefficients for Ni^{2+}. The R_L values (Table II) show that the adsorption behavior of Ni^{2+} onto Reactive Red 120 attached poly(HEMA–EDMA) beads was favorable ($R_L < 1$).

Freundlich plots of Ni^{2+} ions at 20, 30, and 40°C on Reactive Red 120 attached poly(HEMA–EDMA) at pH 6.0 are given in Figure 12. The Freundlich isotherm constants are given in Table II. High correlation coefficients ($R^2 > 0.990$) and the magnitude of the exponent, n, indicated the favorability and capacity of the adsorbent/adsorbate system. The values of n were $1 < n < 10$, which indicated that adsorption was favorable.[35] The Langmuir model makes several assumptions, such as monolayer coverage and constant adsorption energy, whereas the Freundlich equation deals with physicochemical adsorption on heterogeneous surfaces. The applicability of both Langmuir and Freundlich isotherms to Reactive Red 120 attached poly(HEMA–EDMA) beads implies that both monolayer adsorption and heterogeneous surface conditions exist under the experimental conditions used.

TABLE I
Adsorption Kinetic Constants of Ni^{2+} Ions

	Pseudo-first-order kinetic constants	
T (°C)	$K_1 \times 10^3$ (l/min)	R^2
20	11.60	0.993
30	7.60	0.979
40	7.14	0.992

TABLE II
Freundlich and Langmuir Constants for the Adsorption of Ni^{2+} Ions

	Freundlich constants			Langmuir constants			
T (°C)	K_F	n	R^2	b (L/mg)	Q_0 (mg/g)	R^2	R_L
20	0.588	1.775	0.994	0.0855	9.88	0.984	0.163
30	0.514	1.835	0.999	0.0825	8.42	0.984	0.168
40	0.407	1.732	0.992	0.0782	7.43	0.996	0.176

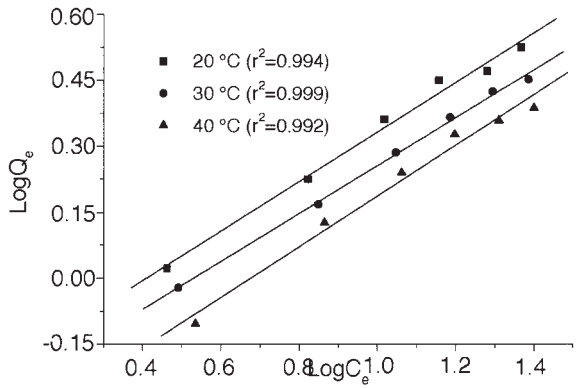

Figure 12 Freundlich plots of Ni^{2+} at 20, 30, and 40°C on Reactive Red 120 attached poly(HEMA–EDMA) beads (dye loading = 25.5 μmol/g, pH = 6.0).

The adsorption properties of the Reactive Red 120 attached poly(HEMA–EDMA) beads are thus likely to be complex, involving more than one mechanism.

Thermodynamic parameters

The thermodynamic parameters for the adsorption of Ni^{2+} onto Reactive Red 120 attached poly(HEMA–EDMA) were calculated with the following equations, and the results of these parameters are given in Table III:

$$\Delta G^0 = -RT \ln b \tag{7}$$

where ΔG^0 is the Gibbs free energy change, R is the gas constant, and T is the temperature. This equation can be rewritten as follows:

$$\ln b = -(\Delta G^0/R)(1/T) \tag{8}$$

The linear change of ln b with $1/T$ has been proven in a number of studies for heavy-metal adsorption by some materials (Fig. 13).[36,37] Activation energy, E_a, can be determined from the slope of ln b versus $1/T$.

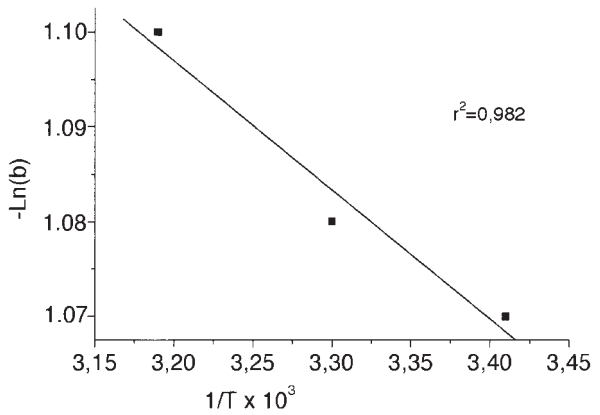

Figure 13 Ln b versus $1/T$ for the adsorption of Ni^{2+} ions to determine the Gibbs free energy.

TABLE III
Thermodynamic Parameters for Ni^{2+} Ions

T (°C)	ΔG^0 (kJ/mol)	ΔH^0 (kJ/mol)	ΔS^0 (J/mol K)	ΔE_a (kJ/mol)
20		2.64	−0.15	
30	−1.13	4.22	−0.31	−2.24
40	—	—	—	—

$$\Delta H^0 = R(T_2T_1/T_2 - T_1) \ln(b_2/b_1) \tag{9}$$

$$\Delta S^0 = -(\Delta G^0 - \Delta H^0)/T \tag{10}$$

where ΔH^0 is the enthalpy change ΔS^0 is the entropy change, and b, b_1, and b_2 are equilibrium constants obtained from the Langmuir isotherms at temperatures T, T_1,and T_2, respectively. As can be seen in Table III, a negative ΔG^0 value indicates the feasibility of the process and the spontaneous nature of adsorption. ΔH^0 was calculated by eq. (9) between 20 and 30°C and between 30 and 40°C.

CONCLUSIONS

Poly(HEMA–EDMA) beads having a swelling ratio of 55% were prepared by the suspension copolymerization of HEMA and EDMA. A metal-chelating dye ligand, that is, Reactive Red 120, was then attached to these beads with a concentration of 25.5 μmol/g of polymer. The adsorption/desorption of Ni^{2+} ions from aqueous media on these beads led to the following conclusions: the Ni^{2+}-ion adsorption was rapid, and adsorption equilibria were reached in about 60 min. The adsorption capacity of the affinity beads from aqueous solutions was 9.88 mg/g for Ni^{2+} ions batchwise. Adsorbed metal ions were easily desorbed with 0.1*M* HNO_3 (pH 1.0). The intraparticle diffusion rate constants at various temperatures were calculated as $k_{20°C}$ = 0.565 mg/g $min^{0.5}$, $k_{30°C}$ = 0.560 mg/g $min^{0.5}$, and $k_{40°C}$ = 0.385 mg/g $min^{0.5}$. When the intraparticle diffusion rate constants were compared, inverse proportionality was observed. Consecutive adsorption and desorption showed the feasibility of this novel affinity microbead for Ni^{2+} adsorption. The equilibrium data fitted very well both Langmuir and Freundlich adsorption models. The pseudo-first-order kinetic model was used to describe the kinetic data.

References

1. Cangul, H.; Broday, L.; Salnikow, K. Toxicol Lett 2002, 127, 69.
2. Kasprzak, K. S.; Sunderman, F. W., Jr.; Salnikow, K. Mutat Res 2003, 533, 67.

3. Kasprzak, K. S. Cancer Inv 1995, 13, 411.
4. Bal, W.; Kozowski, H. K.; Kasprzak, K. S. J Inorg Biochem 2000, 79, 213.
5. Higgings, T. E.; Sater, V. E. Eng Prog 1984, 3, 12.
6. Jansson-Chaprie, M.; Guibal, B.; Roussy, J.; Delanghe, B.; Lecloirec, P. Water Res 1995, 30, 465.
7. Mellah, A.; Chegrohche, S. Water Res 1997, 31, 621.
8. Say, R.; Tuncel, A.; Denizli, A. J Appl Polym Sci 2002, 83, 2467.
9. Denizli, A.; Salih, B.; Piskin, E. React Funct Polym 1996, 29, 11.
10. Van Berkel, P. M.; Driessen, W. L.; Parlevliet, F. J.; Reedijk, J.; Sherrington, D. C. Eur Polym J 1997, 33, 129.
11. Denizli, A.; Şenel, S.; Alsancak, G.; Tüzmen, N.; Say, R. React Funct Polym 2003, 55, 121.
12. Arpa, Ç.; Sağlam, A.; Bektaş, S.; Patır, S.; Genç, Ö.; Denizli, A. Adsorp Sci Technol 2002, 20, 203.
13. Say, R.; Garipcan, B.; Emir, S.; Patır, S.; Denizli, A. Macromol Mater Eng 2002, 287, 539.
14. Denizli, A.; Şatıroğlu, N.; Patır, S.; Bektaş, S.; Genç, Ö. J Macromol Sci Pure Appl Chem 2000, 37, 1647.
15. Denizli, A.; Kocakulak, M.; Pişkin, E. J Macromol Sci Pure Appl Chem 1998, 35, 137.
16. Langmuir, I. J Am Chem Soc 1918, 40, 1361.
17. Freundlich, H. M. F. Z Phys Chem A 1906, 57, 385.
18. Mc Kay, G.; Blair, H. S.; Gardner, J. R. J Appl Polym Sci 1982, 27, 3043.
19. Lagergren, S. K. Svenska Vetenskapsakad Handl 1898, 24, 1.
20. Mc Kay, G.; Ho, Y. S. Process Biochem 1999, 34, 451.
21. Ho, Y. S.; Ofomaja, A. E. J Hazard Mater, in press.
22. Say, R.; Emir, S.; Garipcan, B.; Patır, S.; Denizli, A. Adv Polym Technol 2003, 22, 355.
23. Veglio, F.; Esposito, A.; Reverberi, A. P. Hydrometallurgy 2002, 65, 43.
24. Gupta, R. K.; Singh, R. A.; Dubey, S. S. Sep Purif Technol 2004, 38, 225.
25. Zhou, D.; Zhang, L.; Zhou, J.; Guo, S. Water Res 2004, 38, 2463.
26. Latha, A. G.; George, B. K.; Kannon, K. G.; Ninan, K. N. J Appl Polym Sci 1991, 43, 1159.
27. Li, N.; Bai, R. Sep Purif Technol 2005, 42, 237.
28. Konishi, Y.; Asai, S. S.; Midoh, Y.; Oku, M. Sep Sci Technol 1993, 28, 1691.
29. Denizli, A.; Garipcan, B.; Karabakan, A.; Şenöz, H. Mater Sci Eng C 2005, 25, 448.
30. Liu, R.; Zhang, B.; Tang, H. J Appl Polym Sci 1998, 70, 7.
31. Denizli, A.; Şanlı, N.; Garipcan, B.; Patır, S.; Alsancak, G. Ind Eng Chem Res 2004, 43, 6095.
32. Liu, C. Y.; Chang, H. T.; Hu, C. C. Inorg Chim Acta 1990, 172, 151.
33. Morris, M. E.; Vincent, B.; Snowden, M. J. J Colloid Interface Sci 1997, 190, 198.
34. Allen, S. J.; McKay, G.; Khader, K. Y. H. Environ Pollut 1989, 56, 39.
35. Wu, F. C.; Tseng, R. L.; Juang, R. S. Water Res 2001, 35, 613.
36. Anirudhan, T. S.; Sreedhar, M. K. Indian J Chem Technol 1998, 5, 41.
37. Raji, C.; Anirudhan, T. S. Indian J Chem Technol 1996, 3, 345.